

Quantum phases of atomic boson-fermion mixtures in optical lattices

Robert Roth

Institut für Kernphysik, Technische Universität Darmstadt, 64289 Darmstadt, Germany

Keith Burnett

*Clarendon Laboratory, Department of Physics, University of Oxford,
Parks Road, Oxford OX1 3PU, United Kingdom*

(Dated: November 6, 2018)

The zero-temperature phase diagram of a binary mixture of bosonic and fermionic atoms in an one-dimensional optical lattice is studied in the framework of the Bose-Fermi-Hubbard model. By exact numerical solution of the associated eigenvalue problems, ground state observables and the response to an external phase twist are evaluated. The stiffnesses under phase variations provide measures for the boson superfluid fraction and the fermionic Drude weight. Several distinct quantum phases are identified as function of the strength of the repulsive boson-boson and the boson-fermion interaction. Besides the bosonic Mott-insulator phase, two other insulating phases are found, where both the bosonic superfluid fraction and the fermionic Drude weight vanish simultaneously. One of these double-insulator phases exhibits a crystalline diagonal long-range order, while the other is characterized by spatial separation of the two species.

Following the seminal experiments on the superfluid to Mott-insulator transition in ultracold atomic Bose gases in optical lattice potentials [1, 2], a new frontier in the field of degenerate, strongly correlated quantum gases has emerged. It has recently become possible to prepare degenerate mixtures of a bosonic and a fermionic atomic species in an optical lattice [3]. These degenerate gases will facilitate the experimental study of quantum phase transitions in systems of mixed quantum statistics, which are extremely hard to access in the solid-state context. The superior experimental control available in ultracold atomic gases experiments promises detailed insights into the rich physics of quantum phase transitions. In this paper we explore the phase diagram of a binary boson-fermion mixture in an optical lattice and identify experimental signatures of the different phases.

A theoretical framework for degenerate boson-fermion mixtures in optical lattices can be constructed by a straight-forward generalization of the single-band Bose-Hubbard model, used successfully to describe the superfluid to Mott-insulator phase transition in purely bosonic systems [4]. A complete single-particle basis within the lowest Bloch band is given by the Wannier functions for the vibrational ground state of each lattice well. We define creation operators \hat{a}_i^\dagger (\hat{c}_i^\dagger) which create a boson (fermion) in the localized Wannier state at site $i = 1, \dots, I$. Using this basis we can translate the many-body Hamiltonian into a second quantized form. This leads to the Bose-Fermi-Hubbard (BFH) Hamiltonian for a one-dimensional translationally invariant lattice [5, 6, 7]

$$\begin{aligned} \hat{H} = & -J_B \sum_{i=1}^I (\hat{a}_{i+1}^\dagger \hat{a}_i + \text{h.a.}) - J_F \sum_{i=1}^I (\hat{c}_{i+1}^\dagger \hat{c}_i + \text{h.a.}) \\ & + \frac{V_{BB}}{2} \sum_{i=1}^I \hat{n}_i^B (\hat{n}_i^B - 1) + V_{BF} \sum_{i=1}^I \hat{n}_i^B \hat{n}_i^F, \end{aligned} \quad (1)$$

where $\hat{n}_i^B = \hat{a}_i^\dagger \hat{a}_i$ and $\hat{n}_i^F = \hat{c}_i^\dagger \hat{c}_i$ are the occupation number operators for bosons and fermions, respectively. The first line describes the tunneling between adjacent lattice sites. The tunneling amplitudes J_B and J_F are connected to off-diagonal matrix elements of the kinetic energy and the lattice potential [5]. The second line of Eq. (1) contains the on-site boson-boson and boson-fermion interactions with interaction strengths V_{BB} and V_{BF} , respectively. Within the single-band approximation a fermion-fermion on-site interaction does not arise as the Pauli principle prevents two identical fermions from occupying the same site.

We exactly solve the eigenvalue problem of the BFH Hamiltonian within a complete basis of Fock states of the form $|\{n_1^B, \dots, n_I^B\}_\alpha\rangle \otimes |\{n_1^F, \dots, n_I^F\}_\beta\rangle$. By $\{n_1^B, \dots, n_I^B\}_\alpha$ we denote a set of boson occupation numbers for the individual sites. The index $\alpha = 1, \dots, D_B$ labels all possible compositions of occupation numbers which yield $\sum_{i=1}^I n_i^B = N_B$. For the set of fermion occupation numbers $\{n_1^F, \dots, n_I^F\}_\beta$ only those compositions with 0 or 1 fermions at a given site are allowed by the Pauli principle. The dimensions of the boson and fermion space are given by $D_B = (N_B + I - 1)! / (N_B! (I - 1)!)$ and $D_F = I! / (N_F! (I - N_F)!)$, respectively. For a lattice with $I = 8$ sites, $N_B = 8$ bosons, and $N_F = 4$ fermions the basis dimensions are $D_B = 6435$ and $D_F = 70$. Clearly, the dimension of the fermion space is dramatically reduced due to the Pauli principle.

Within the basis of Fock-states we construct the matrix representation of the BFH Hamiltonian assuming periodic boundary conditions. The lowest eigenvalues and eigenvectors of the Hamilton matrix are computed using a refined Lanczos algorithm. The eigenvectors provide the coefficients for the representation of the eigenstates

$|\Psi_\nu\rangle$ in the Fock-state basis

$$|\Psi_\nu\rangle = \sum_{\alpha=1}^{D_B} \sum_{\beta=1}^{D_F} C_{\alpha\beta}^{(\nu)} |\{n_1^B, \dots, n_I^B\}_\alpha\rangle \otimes |\{n_1^F, \dots, n_I^F\}_\beta\rangle. \quad (2)$$

From this representation of the ground state we can extract various observables such as mean occupation numbers and number fluctuations for both species. It also provides access to more elaborate quantities such as the one- or two-body density matrix and the static structure factor, which we will discuss below.

The dynamical response of the system to external perturbations is a crucial quantity in distinguishing between different quantum phases, for example, between the bosonic Mott-insulator and the superfluid phase. By imposing a linear variation of the phase onto the many-body wavefunction one can probe the mobility of the atoms in the lattice. On the single particle level, a spatial variation of the phase of the wavefunction is associated with a velocity field $\vec{v}(\vec{x}) = \frac{\hbar}{m} \vec{\nabla} \theta(\vec{x})$, and a linear phase variation thus corresponds to a constant velocity across the lattice. Roughly speaking, those particles free to move will respond to the phase twist and exhibit a homogeneous flow. This flow is then associated with an additional kinetic energy and hence an increase of the total energy. This provides a measure for the density of mobile particles in the lattice [8, 9].

This phase variation can be realized by imposing twisted boundary conditions for the many-body wavefunction. In the case of the BFH model it is, however, more convenient to map the phase twist by means of a unitary transformation onto the Hamiltonian [8]. This leads to a ‘‘twisted’’ Hamiltonian which contains Peierls phase factors in the hopping terms:

$$\begin{aligned} \hat{H}_{\Theta_B, \Theta_F} = & -J_B \sum_{i=1}^I (e^{-i\Theta_B/I} \hat{a}_{i+1}^\dagger \hat{a}_i + \text{h.a.}) \\ & -J_F \sum_{i=1}^I (e^{-i\Theta_F/I} \hat{c}_{i+1}^\dagger \hat{c}_i + \text{h.a.}) \\ & + \frac{V_{BB}}{2} \sum_{i=1}^I \hat{n}_i^B (\hat{n}_i^B - 1) + V_{BF} \sum_{i=1}^I \hat{n}_i^B \hat{n}_i^F. \end{aligned} \quad (3)$$

In order to probe the response of the bosonic and the fermionic species separately, we have introduced different total twist angles Θ_B and Θ_F , respectively.

For an isolated boson twist ($\Theta_B > 0, \Theta_F = 0$) the difference in the ground state energies of the boson-twisted Hamiltonian $\hat{H}_{\Theta_B, 0}$ and the initial Hamiltonian $\hat{H}_{0, 0}$ provides direct information on the superfluid density of the bosonic component. This is because the superfluid component responds to the imposed phase gradient producing flow and the associated energy change. The bosonic phase stiffness

$$f_s^B = \frac{I^2}{N_B J_B} \frac{E_{\Theta_B, 0} - E_{0, 0}}{\Theta_B^2}, \quad \Theta_B \ll \pi \quad (4)$$

is, therefore, a measure for the boson superfluid fraction [8, 9, 10, 11]. We note that neither the stability of the superflow nor the reduction of the flow by the lattice itself are taken into account by this quantity. The superfluid weight f_s^B vanishes for insulating phases such as the Mott-insulator phase and goes to 1 for a perfect superfluid.

The energy change resulting from an isolated fermion twist ($\Theta_B = 0, \Theta_F > 0$) provides a measure for the mobility of the fermionic atoms. The fermionic phase stiffness

$$f_d^F = \frac{I^2}{N_F J_F} \frac{E_{0, \Theta_F} - E_{0, 0}}{\Theta_F^2}, \quad \Theta_F \ll \pi \quad (5)$$

is equivalent to the well-known Drude weight for charged fermions in a lattice [12, 13, 14]. The vanishing of the Drude weight is an indicator of an insulating state, whereas a finite value indicates non-vanishing conductivity.

These two phase stiffnesses are an important tool to characterize the different quantum phases of the boson-fermion mixture in a lattice. In the following we map out the phase diagrams for different boson and fermion numbers, N_B and N_F , as function of the strength of the repulsive boson-boson and the boson-fermion interaction. For simplicity we examine the case of equal tunneling rates for the two species, i.e. $J = J_B = J_F$, and use J as energy unit. The only remaining parameters of BFH Hamiltonian are then the ratios between the two interaction strengths and the tunneling rate, V_{BB}/J and V_{BF}/J . For each point in the V_{BB} - V_{BF} -plane we solve the eigenvalue problem of the BFH Hamiltonian (1) and the two twisted Hamiltonians $\hat{H}_{\Theta_B, 0}$ and \hat{H}_{0, Θ_F} (with $\Theta_B, \Theta_F = 0.1$) in order to compute the phase stiffnesses and several simple ground state observables.

First we consider a lattice with $I = 8$ sites and equal filling factors $N_B/I = 1/2$ and $N_F/I = 1/2$ for the bosonic and the fermionic species, respectively. Although the system is rather small we could confirm that finite size effects are insignificant for the observables discussed in the following [8]. Figure 1 shows contour plots of the boson stiffness f_s^B , i.e., the superfluid fraction within the bosonic species, and the fermion stiffness f_d^F , i.e., the Drude weight for the fermionic component. In addition the largest coefficient C_{\max}^2 of the expansion (2) of the ground state is given. Large values of C_{\max}^2 indicate that the ground state is dominated by one or a few particular Fock states.

Figures 1(a) and (b) reveal that in the large parameter region for $V_{BB}/J \gtrsim 5$ and $V_{BF}/J \gtrsim 15$ the boson and the fermion phase stiffnesses vanish. The bosonic and the fermionic components then behave like insulators, i.e., the superfluid fraction and the Drude weight are both zero. This double-insulator phase is generated by the combined action of the boson-boson and the boson-fermion repulsion. Any configuration which has two bosons or a boson and a fermion at the same site is energetically unfavorable, and the ground state is

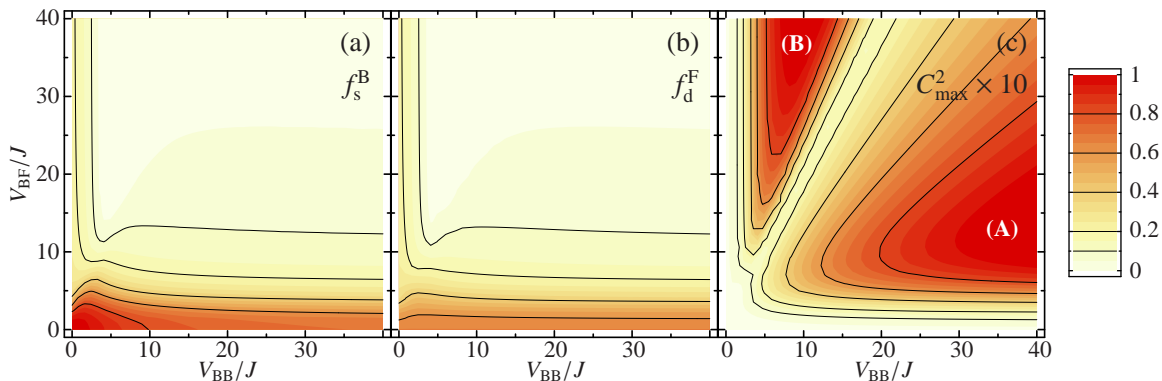


FIG. 1: Contour plots of (a) the bosonic superfluid fraction f_s^B , (b) the fermionic Drude weight f_d^F , and (c) the largest coefficient C_{\max}^2 as function of V_{BB}/J and V_{BF}/J for a lattice with $I = 8$ sites and $N_B = N_F = 4$.

therefore dominated by Fock states with either one boson or one fermion per site. Only if one of the interaction strengths is small can a finite stiffnesses for bosons and fermions emerge.

Closer inspection of the largest coefficient of the expansion (2), displayed in Fig. 1(c), reveals that within the double-insulating region there are two distinct areas where the largest coefficient reaches $C_{\max}^2 \approx 0.1$. Hence there is a class of Fock states which provide the dominant contribution to the ground state. In region (A) for values $2V_{BB} \gtrsim V_{BF}$ the dominant Fock states exhibits an alternating occupation of the sites with one boson or one fermion. In region (B) the dominant Fock states contain a continuous block of bosons followed by a block of fermions. Note that although these states have the largest weight, other Fock states do also contribute to the ground state. Most important are those which can be generated from the dominant Fock state by exchange of two lattice sites or particle-hole excitations.

The reason for the existence of and the cross-over between these two different intrinsic structures is quite subtle. All the interaction matrix elements for the dominant Fock states are irrelevant, because all these states have exactly one particle (boson or fermion) at each site. The existence of the two different structures is triggered by states with double occupancies that enter into the ground state with much smaller weight but nevertheless couple to the dominant states via the tunneling term. This complex correlation dictates the cross-over between alternating and separated species.

A good observable to distinguish the different intrinsic configurations is the static structure factor [8]. For the bosonic component it is given by

$$S^B(ka) = \frac{1}{N_B^2} \sum_{i,j=1}^I e^{ika(i-j)} \langle \Psi_0 | \hat{n}_i^B \hat{n}_j^B | \Psi_0 \rangle, \quad (6)$$

where a is the lattice spacing. It measures the density-density correlations in the system and thus provides information on the presence or otherwise of diagonal long-range order.

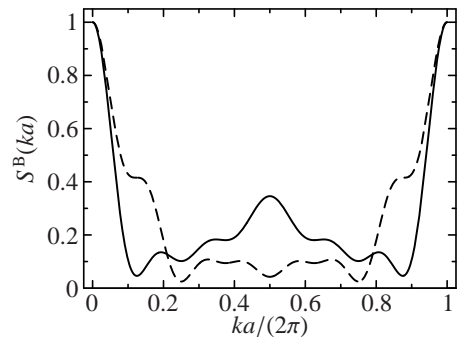


FIG. 2: Static structure factor $S^B(ka)$ for $I = 8$ and $N_B = N_F = 4$ as function of ka for the ground state with alternating occupation at $V_{BB}/J = 40$, $V_{BF}/J = 15$ (solid line) and with separated species for $V_{BB}/J = 10$, $V_{BF}/J = 40$ (dashed line).

Figure 2 shows an example for the structure factor within the region of alternating occupation (full line) and the region of phase separation (dashed line). Apart from the trivial peaks at integer multiples of 2π the structure factor differs substantially within the two phases. For the alternating occupation phase, $S^B(ka)$ exhibits an enhancement around $ka = \pi$ which signals an increased probability for a boson to be found at every other site. This is the signature of diagonal long-range order as it is found in a crystal. In a two-dimensional lattice the corresponding checkerboard configuration, which exhibits crystalline diagonal long-range order, was identified recently [7].

Within the separated phase the structure factor shows a rather different behavior (dashed line in Fig. 2): it is suppressed around $ka = \pi$ and enhanced at $ka \approx 2\pi/I$. Due to this difference in the structure factors it might be possible to distinguish the two types of double-insulator phases experimentally, e.g., through selective Bragg diffraction of light off the trapped atoms. We note that the interference pattern produced by the atoms after release from the lattice, along with ballistic expansion, will not distinguish the phases as their coherence properties, i.e., the off-diagonal long-range order, are too similar.

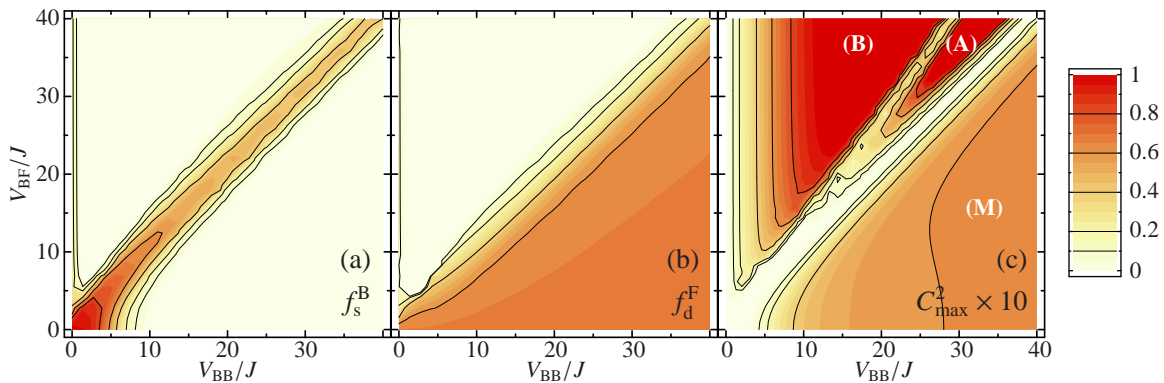


FIG. 3: Contour plots of (a) the bosonic superfluid fraction f_s^B , (b) the fermionic Drude weight f_d^F , and (c) the largest coefficient C_{\max}^2 as function of V_{BB}/J and V_{BF}/J for a lattice with $I = 8$ sites, $N_B = 8$, and $N_F = 4$.

As a second example we consider a lattice with $I = 8$ sites, a boson filling factor $N_B/I = 1$, and a fermion filling factor $N_F/I = 1/2$. Contour plots of the bosonic and fermionic stiffness and the largest coefficient as function of V_{BB}/J and V_{BF}/J are shown in Fig. 3.

The qualitative difference compared to the half-filling case is the appearance of a bosonic Mott-insulator phase (M) for $V_{BB} > V_{BF}$. In this region the boson stiffness, i.e. the superfluid fraction, vanishes whereas the fermionic stiffness remains at its noninteracting value as depicted in Figs. 3(a) and (b). Under the influence of the strong boson-boson repulsion the bosons form a Mott insulating layer. The fermions are not affected, they experience a homogeneous background of bosons on which they can move freely.

The situation changes if the boson-fermion interaction becomes comparable in strength to the boson-boson interaction. Through the boson-fermion repulsion the fermions are able to break up the bosonic Mott-insulator and partially restore bosonic superfluidity in the region $V_{BF} \approx V_{BB}$. Further increase of the boson-fermion repulsion leads to the simultaneous reduction of both phase stiffnesses and to the formation of a double-insulator regime as observed in the case of half-filling. The contour plot for the largest coefficient C_{\max}^2 depicted in Fig. 3(c) reveals that both of the previously observed intrinsic configurations appear again: (A) an alternating occupation of the sites associated with crystalline diago-

nal long-range order and (B) continuous blocks of bosons and fermions which resemble a spatial separation of the two components. Due to the appearance of the bosonic Mott-insulator both phases have been shifted to the region $V_{BF} > V_{BB}$.

In summary, we have mapped out the phase diagrams of a binary mixture of bosonic and fermionic atoms in a one-dimensional lattice. By exact numerical solution of the eigenvalue problem for the Bose-Fermi-Hubbard Hamiltonian we are able to compute ground states as well as the dynamical response of the system. The stiffnesses of the bosonic and fermionic component under phase twists provides an important measure for the superfluid properties of the bosonic component (superfluid fraction) and the conductivity of the fermionic species (Drude weight). Using these quantities we have identified several distinct quantum phases, e.g., a bosonic Mott-insulator phase and two double-insulator phases which exhibit different degrees of diagonal long-range order—alternating occupation and component separation. This shows that atomic boson-fermion mixtures in optical lattices constitute a versatile tool for the study of fundamental quantum phase transitions.

This work was supported by the DFG, the UK EPSRC, and the EU via the “Cold Quantum Gases” network. K.B. thanks the Royal Society and Wolfson Foundation for support.

-
- [1] M. Greiner *et al.*, Nature **415**, 39 (2002).
 [2] M. Greiner *et al.*, Nature **419**, 51 (2002).
 [3] G. Modugno *et al.*, Phys. Rev. A **68**, 011601(R) (2003).
 [4] D. Jaksch *et al.*, Phys. Rev. Lett. **81**, 3108 (1998).
 [5] A. Albus, F. Illuminati, and J. Eisert, Phys. Rev. A **68**, 023606 (2003).
 [6] M. Lewenstein *et al.*, (2003), cond-mat/0306180.
 [7] H. P. Büchler and G. Blatter, Phys. Rev. Lett. **91**, 130404 (2003).
 [8] R. Roth and K. Burnett, Phys. Rev. A **68**, 023604 (2003).
 [9] R. Roth and K. Burnett, Phys. Rev. A **67**, 031602(R) (2003).
 [10] M. E. Fisher, M. N. Barber, and D. Jasnow, Phys. Rev. A **8**, 1111 (1973).
 [11] W. Krauth, Phys. Rev. B **44**, 9772 (1991).
 [12] D. J. Scalapino, S. R. White, and S. Zhang, Phys. Rev. B **47**, 7995 (1993).
 [13] R. M. Fye *et al.*, Phys. Rev. B **44**, 6909 (1991).
 [14] B. S. Shastry and B. Sutherland, Phys. Rev. Lett. **65**, 243 (1990).